Molecular Vision 2019; 25:714-721 <http://www.molvis.org/molvis/v25/714>
Received 11 December 2018 | Accepted 10 November 2019 | Published 14 November 2019

Evidence of the involvement of dystrophin Dp71 in corneal angiogenesis

Gabriella Ortiz,[1] Ophélie Vacca,[2] Romain Bénard,[3] Bénédicte Dupas,[4] Florian Sennlaub,[3] Xavier Guillonneau,[3] Sahel JA,[3, 5, 6] Ramin Tadayoni,[3, 4] Alvaro Rendon,[3] Audrey Giocanti-Aurégan[3, 7]

[1]Sussex Eye Hospital - Brighton and Sussex University Hospitals, NHS Trust, UK; [2]Neuroscience Paris-Saclay Institute (Neuro-PSI), Université Paris Sud, CNRS, Université Paris Saclay, Orsay, France; [3]Institut De La Vision, Sorbonne Universités, UPMC Univ Paris 06, UMR_S, 968, Paris, France, Paris, France; [4]Ophthalmology Department, Hôpital Lariboisière, AP-HP, Université Paris 7, Sorbonne Paris Cité, 2 Rue Ambroise Paré, Paris, 75010, France; [5]Centre Hospitalier National d'ophtalmologie Des Quinze-Vingts, DHU View Maintain, Paris, France; [6]Fondation Ophtalmologique Rothschild, Paris, France; [7]Ophthalmology department, Avicenne hospital, DHU vision and handicaps, 125 rue de Stalingrad, Bobigny

Purpose: The aim of this study was to define the role of dystrophin Dp71 in corneal angiogenesis.
Methods: Inflammation-induced corneal neovascularization experiments were performed in *Dp71*-null mice and C57BL/6J wild-type mice.
Results: The corneal neovascular area covered by neovascularization was larger in the injured corneas of the *Dp71*-null mice compared to the corneas of the wild-type mice: 40.72% versus 26.33%, respectively ($p<0.005$). Moreover, increased angiogenesis was associated with a high expression of vascular endothelial growth factor (VEGF). Similarly, aortic ring assays showed a significant enhancement of the neovascular area.
Conclusions: These results suggest that dystrophin Dp71 could play an important role as a negative regulator of corneal angiogenesis.

The formation of new blood vessels, referred to as angiogenesis, is an important process in health and disease. In healthy eyes, angiogenesis occurs during development; however, under pathological conditions, angiogenesis is involved in many diseases. The cornea is an avascular and transparent tissue, the clarity of which is partly due to the absence of blood vessels, resulting from a very complex and regulated system of proangiogenic and antiangiogenic molecules. Corneal injury leading to inflammation is associated with corneal angiogenesis, which leads to tissue healing, edema, and reduced visual acuity, and is often sight-threatening [1]. Substantial evidence indicates that the upregulation of vascular endothelial growth factor (VEGF) and its receptors plays a central role in angiogenesis.

We report evidence suggesting the implication of dystrophin Dp71 in corneal angiogenesis. Dp71 is a protein that belongs to the dystrophin family coded by the *Duchenne muscular dystrophy* (*DMD*; OMIM 300377) gene. Dystrophins are cytoskeleton membrane-associated proteins that are the core of a protein complex (dystrophin-associated proteins, DAPs) binding the extracellular matrix (ECM) to the actin cytoskeleton [1]. Different promoters can influence *DMD* gene expression, and dystrophins other than Dp71, such as Dp427, Dp260, Dp140, and Dp116, may be expressed [2]. Dp71 is mainly found in non-muscular tissues [3], and it is the most abundant dystrophin in the central nervous system and in the retina, where Dp71 is mainly located in the inner limiting membrane, in Müller glial cell endfeet [4,5], in retinal astrocytes [6] surrounding vessels, and in the crystalline lens [7]. Using *Dp71*-null mice, we recently showed that Dp71 regulates astrocyte morphology, and appears to be a key component in the proper development of retinal vessels after birth [6]. We have also shown that the deletion of *Dp71* was associated with increased VEGF expression and vascular inflammation [8] in the retina.

Because corneal neovascularization is a well-established model system in vivo for studying angiogenesis, the aim of this study was to assess whether Dp71 could play a regulatory role in the cornea, an eye tissue devoid of macroglial cells, using this model. Corneal angiogenesis was induced by corneal epithelial injury after mechanical scratching to determine whether the absence of Dp71 could change the angiogenic response. Additionally, aortic rings obtained from *Dp71*-null mice were used to confirm the presence of Dp71 in vessel-like extensions from explants. The results showed that Dp71 could act as a negative regulator of neoangiogenesis in the cornea.

Correspondence to: Alvaro Rendon; Institut de la Vision, 17 rue Moreau 75012 Paris, France; Phone: 0153462565; FAX: 0153462570; email: alvaro.rendon@inserm.fr

METHODS

Animal model: All experiments were performed in compliance with the European Community Council Directives, France (86/609/EEC) for animal care and experimentation (HMG). Mice were handled in accordance with the ARVO Statement for the Use of Animals in Ophthalmic and Vision Research (IOVS). *Dp71*-null mice were obtained as described previously [9], by replacing the first and unique exon of *Dp71* and a small part of its first intron by a sequence encoding a β-galactosidase (β-gal)-neomycin-resistance chimeric protein (β-geo). This abolishes the expression of *Dp71*, and the inserted promotorless *β-geo* gene is expressed under the control of the *Dp71* promoter. *Dp71*-null mice and their littermates (C57BL6) were bred in our laboratory. The mice were identified with analysis of the PCR products using the following oligonucleotide primers: *Dp71* (forward), 5′-ATG AGG GAA CAG CTC AAA GG-3′ and *Dp71* (reverse), 5′-TGC AGC TGA CAG GCT CAA GA-3′. PCR amplification consisted of an initial denaturation step at +95 °C for 10 min, followed by 40 cycles of denaturation at +95 °C for 15 s and annealing and extension at +60 °C for 1 min. Melting curve analysis (+60 °C to +95 °C increment at +0.3 ºC) was used to determine the melting temperature of specific amplification products and the possible formation of primer dimers.

Model of corneal neovascularization and immunostaining: All mice used for inflammation-induced corneal neovascularization experiments were 8 weeks of age. The mice were topically anesthetized with tetracaine 1% (FAURE), and 2 µl of 0.15 M NaOH were applied to the right cornea of each mouse for 30 s. Then the cornea was dried. The corneal and limbal epithelia were removed by scraping with a 45° Microsurgical Knife (Sharpoint, Cheshire, UK) [10]. One person (GO, a cornea specialist) performed the scraping, and applied the same strength to the entire cornea. Rifamycin Chibret (Théa Laboratory, Clermont-Ferrand, France) was instilled immediately after epithelial denudation in the right eye (the studied eye), and Ocryl-Gel (TVM, Lempdes, France) was applied on the left cornea (the control eye). The mice were euthanized by cervical dislocation 7 days after the corneal injury when the cornea neovascularization was the maximum [11]. Vascular endothelial cells were visualized with immunostaining of the flatmounted corneas with fluorescein isothiocyanate (FITC)-conjugated anti-CD31 antibodies. For PBS preparation, we started with 800 ml of distilled water, added 8 g of NaCl, 0.2 g of KCl, 1.44 g of Na_2HPO_4, 0.24 g of KH_2PO_4 and adjusted the pH to 7.4 with HCl and added distilled water to a total volume of 1 l. Fresh corneas were dissected, rinsed in 0.1 M PBS for 30 min, and fixed in 100% ice-cold acetone for 20 min. After the specimens were washed in 0.1 M PBS, the nonspecific binding was blocked with 0.1 M PBS and 2% bovine serum albumin (BSA; Sigma-Aldrich, Darmstadt, Germany) for 1 h at room temperature. Incubation with FITC-conjugated anti-CD31 antibodies (1:300; BD Pharmingen, San-Jose, CA) in 0.1 M PBS and 2% BSA at 4 °C overnight was followed by three washes in 0.1 M PBS at room temperature. The corneas were mounted with PermaFluor (BD Biosciences, San Jose, CA).

Corneal sections: The mice were euthanized at different time points (n=6 animals per group at each time point). The corneas were fixed in 4% paraformaldehyde, transferred to 30% sucrose/PBS overnight at 4 °C, and embedded at optimal cutting temperature (OCT; Cryomatrix, Thermo Scientific, Montigny-Le-Bretonneux, France). Ten-micrometer frozen sections were washed with PBS, and blocked for 1 h with 0.1% Triton-1% BSA-PBS, before overnight incubation at 4 °C with rabbit anti-dystrophin H4 antibodies (1:2,000) [12]. The sections were then incubated with a goat anti-rabbit, goat anti-mouse, and goat anti-rat secondary antibody (1:500; Invitrogen-Molecular Probes, Darmstadt, Germany) for 1 h at room temperature. Cell nuclei were labeled with the nucleic acid dye 4’, 6-diamidino-2-phenylindole (DAPI, 300 nM; Invitrogen-Molecular Probes). In each case, secondary control incubations were performed to determine staining specificity.

Aortic ring angiogenesis assay: Thoracic aortas were removed from 8-week-old mice euthanized with CO_2 asphyxiation, and immediately transferred to a culture dish containing ice-cold endothelial cell basal medium (EGM-2; Cambrex Bio Science, Walkersville, MD). The periaortic fibroadipose tissue was carefully removed with fine microdissecting forceps and scissors, paying special attention not to damage the aortic wall. One-millimeter-long aortic rings (15 per aortas of six wild-type (WT) and *Dp71*-null mice) were sectioned, and rinsed extensively with eight consecutive washes of EGM-2. The rings were then individually embedded in 48-well plates previously coated with 50 µl of synthetic basement membrane (Matrigel; BD Biosciences) per well. After 1 h at 37 °C, 500 µl of EGM-2 were added to each well, and the cultures were incubated at 37 °C for 7 days. The culture medium was changed daily.

X-Gal staining: Tissues were collected and fixed with 4% paraformaldehyde (PAF) for 15 min, and washed three times in PBS for 5 min. A solution prepared in the dark containing X-Gal (diluted at 40 mg/ml in diméthylsulfoxyde [DMSO]), K_4 Fe(CN)$_6$ (200 mM), K3 Fe(CN)$_6$ (200 mM), and MgCl2 (1 M) was added to the tissues. Then the tissues were incubated overnight at 37 °C. Via knock-in, a direct evaluation of

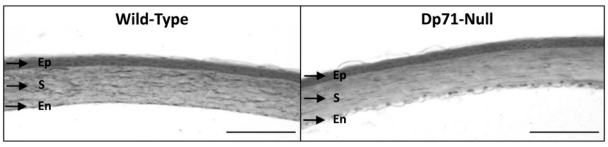

Figure 1. Corneal histology after hematoxylin-eosin staining of tissue sections of WT and *Dp71*-null mice. Both presented an organized corneal histology with the epithelium (Ep), stroma (S), Descemet membrane, and endothelium (En; scale bar=200 µm).

the endogenous activity of the *Dp71* promoter is possible, because this promoter controls *β-gal* gene expression. Using an enzymatic substrate, X-Gal allows blue staining of the cells expressing the reporter gene visible under a white-light microscope.

VEGF measurements with ELISA: The corneas of six mice (n=3 per group) were carefully isolated and placed in 200 µl of RIPA lysis buffer (50 mM Tris-HCl pH 7.2, 150 mM NaCl, 1% Triton, 0.1% sodium dodecyl sulfate (SDS), 0.01% deoxycholate) supplemented with protease inhibitors, and sonicated. The lysate was centrifuged at 19,000 ×g for 10 min at 4 °C. Aliquots (50 µl) of the supernatant were used for VEGF measurements. VEGF was assayed using a sandwich enzyme-linked immunosorbent assay (ELISA) with an affinity-purified polyclonal antibody specific to mouse VEGF and mouse VEGF standard (Quantikine Mouse VEGF Immunoassay, R&D Systems, Rotchester, MN), according to the manufacturer's instructions. VEGF concentrations were normalized to the total protein level.

Electrophoresis, western blotting, and immunodetection: The corneas were homogenized at 4 °C in RIPA extraction buffer supplemented with protease inhibitors, and sonicated. The lysate was centrifuged at 19,000 ×g for 10 min at 4 °C. The protein concentrations were assessed using the Bradford method. Protein extracts were resolved on 4–12% gradient polyacrylamide SDS gels (Invitrogen, Darmstadt, Germany). Then, they were electrotransferred onto a polyvinylidene fluoride (PVDF) membrane (Millipore, Burlington, MA). The blots were blocked with 5% dry milk (Bio-Rad, Hercules, CA) in PBS for 1 h, and then incubated with the primary antibody H4 overnight at 4 °C. After washing, they were probed with a horseradish peroxidase (HRP)-labeled goat anti-rabbit secondary antibody (Interchim, Montluçon, France). Chemiluminescence was finally detected using an electrochemiluminescence (ECL) and western blotting detection system (Amersham Bioscience, Little Chalfont, UK).

Image analysis: To assess vascularization development, images were captured with a fluorescence microscope (Leica Z6 APO Microsystem Inc., Deerfield, IL). The surface area of the flatmounted corneas covered by vessels was measured, and expressed as a percentage of the entire corneal area to obtain the vascularized area. Measurements were made with Photoshop 7.0 software (Adobe, Mountain View, CA).

Statistical analysis: Results are expressed as the mean ± standard error of the mean (SEM). Statistical analyses were performed using a Mann–Whitney test and an ANOVA. A p value of less than 0.05 was considered statistically significant.

RESULTS

Histological analysis and dystrophin location in the corneas of WT and Dp71-null mice: Histological analysis of the corneal sections of the WT and *Dp71*-null mice after hematoxylin-eosin staining (Figure 1) showed that the corneal thickness and the organization of the epithelium, stroma, and Descemet membrane were not impaired in the absence of *Dp71* compared to the WT corneas. However, we observed that the endothelial cells of the *Dp71*-null mice had more vacuoles than the WT mice, suggesting an endothelial dysfunction.

To determine the location of the dystrophins, corneal cross-sections of the WT and *Dp71*-null mice were stained with a pan-specific antibody directed against all the products of the *DMD* gene (Figure 2A). An analysis of the staining of the WT and *Dp71*-null tissues revealed that the immunostaining intensity was higher in the corneal epithelium of the *Dp71*-null mice, while the stromal immunostaining was similar in both groups, and the endothelial immunostaining was strongly reduced. In contrast with this observation, the overall staining density semiquantification showed no statistically significant change between the WT and *Dp71*-null mice (Figure 2B). These results suggest that Dp71 is mainly expressed in the endothelium layer of the cornea.

Dystrophin expression in a corneal injury model of WT and Dp71-null mice: The expression of *DMD* gene products was assessed with western blotting on whole corneal extracts obtained from WT and *Dp71*-null mice after injury in the alkaline-injury model and in the absence of injury. The bands corresponding to dystrophins Dp71, Dp116, and Dp140 were expressed in the corneas of the WT mice (Figure 2C). Beta-actin was used for normalizing the relative expression of the

dystrophins. As expected in the non-injured corneas of the *Dp71*-null mice, only Dp71 expression was absent (Figure 2C), whereas the expression of Dp116 was increased (Figure 2D) and that of Dp140 (Figure 2F) was unchanged. The comparison of the non-injured and injured WT and *Dp71*-null corneas showed that after injury, (i) Dp71 expression (Figure 2E) was unchanged, (ii) Dp116 (Figure 1D) tended to be highly expressed in both strains of mice (statistically significant difference between the WT and *Dp71*-null non-injured mice, *p<0.05), and (iii) Dp140 expression (Figure 1F) was unchanged. These results might suggest that the absence of Dp71 could be compensated by the upregulation of other *DMD* gene products, such as Dp116, in non-injured corneas. There was no statistically significant difference in Dp116 expression between the injured and non-injured *Dp71*-null mice.

Impact of the absence of Dp71 on the corneal angiogenic response to injury: As Dp71 is known to play a crucial role in retinal vascular functions, we investigated whether corneal angiogenesis was impaired in *Dp71*-null mice compared to WT mice. Corneal neovascularization was assessed after the wound-healing process following corneal injury, using flatmounted corneas stained with FITC-conjugated anti-CD31 antibodies. Neovascularization developed centripetally on the cornea from corneal limb vessels, forming a network (Appendix 1) developing toward the corneal center in the WT and *Dp71*-null mice (Figure 3A). The percentage of corneal area covered by neovascularization was larger in the injured corneas of the *Dp71*-null mice than in the corneas of the WT mice: 40.72% versus 26.33%, respectively (p<0.005; Figure 3B). To assess differences in the development of neovascularization between the WT and *Dp71*-null mice, we also assessed the expression of VEGF during the wound-healing process with ELISA, and showed that, in the injured corneas, the level of VEGF was statistically significantly higher in the absence of Dp71 than in the WT corneas (Figure 3C). The process of enhanced neovascularization in the absence of Dp71 suggested that Dp71 could be involved in corneal molecular mechanisms that negatively control angiogenesis.

Expression and location of Dp71 in aortic rings: To determine whether Dp71 was expressed in aortic rings, western blotting was performed on the WT and *Dp71*-null aortic rings (Appendix 2). Dp71 was expressed in the aortic rings of the WT mice and absent in the aortic rings of the *Dp71*-null mice. Furthermore, the X-Gal method described by Sarig et al. [9] that allows quantification of the expression of the reporter *β-gal* gene that replaces Dp71 was used in the aortic rings of the WT and *Dp71*-null mice. β-gal was expressed only in the aortic rings of the *Dp71*-null mice (Supplementary Figure S2A). The staining of β-gal appeared tangential to, and around, the elastic limiting membrane, which suggested that Dp71 was expressed in the smooth muscle fibers of the aortic rings in the WT mice.

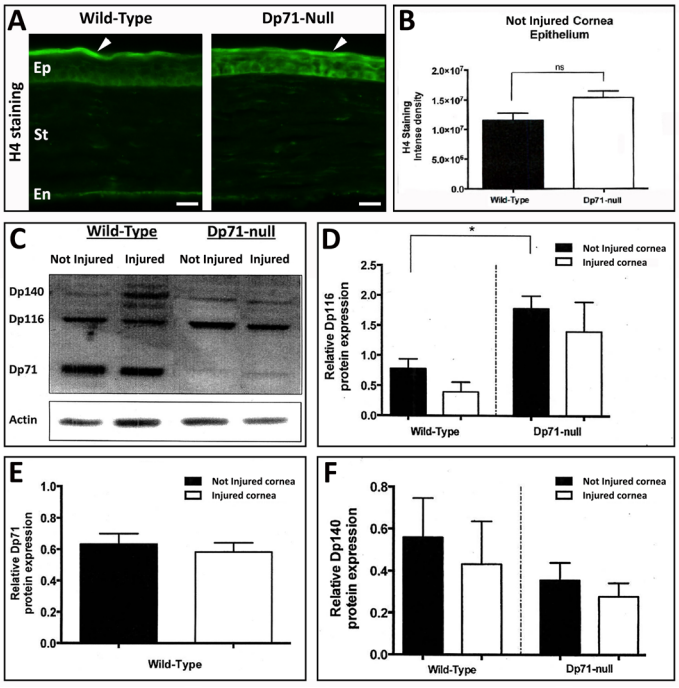

Figure 2. Dystrophin expression after or in the absence of corneal injury. **A**: Immunostaining with a pan-specific antibody directed against dystrophins (H4, green) of the cornea of non-injured wild-type (WT) and *Dp71*-null mice (scale bar=20 µm). **B**: Quantification of H4 staining density with Photoshop software. **C**: Western blotting of dystrophins on injured and non-injured corneal extracts of WT and *Dp71*-null mice. **D**–**F**: Semiquantification of Dp116 (**D**), Dp71 (**E**), and Dp140 (**F**) protein expression relative to β-actin.

Impact of the absence of Dp71 on angiogenesis in Dp71-null mice: To determine the role of Dp71 in the ex vivo aortic ring assay, the angiogenic response of cultured WT and *Dp71*-null aortas was analyzed (Figure 4). The aortic rings of the WT and *Dp71*-null mice were incubated with endothelial basal medium (EBM) for 7 days (Figure 4A). Then, the vascular area surrounding the ring was quantified from day 3 after incubation until day 7. A larger vascular area surrounding the aortic ring was systematically found in the *Dp71*-null mice compared to the WT mice (Figure 4B). The same results were found using EBM in the presence or the absence of VEGF (Figure 4B,C).

DISCUSSION

Corneal angiogenesis is a severe sight-threatening complication of the cornea. It is characterized by an ingrowth of neovessels originating from the limbus, and is often accompanied by an inflammatory response. VEGF is an important factor, because it stimulates corneal neoangiogenesis. Angiogenesis is initiated by the release of proangiogenic factors that attract inflammatory cells. Angiogenesis is controlled through on-and-off switches that can induce the inhibition or the development of the angiogenic process. In a previous work [6] in the mouse retina, we reported that Dp71 plays an important role in physiologic angiogenesis during early development of the retinal vascular plexus sustained by astrocytes. We showed that the deletion of Dp71 statistically significantly reduces vascular growth, as well as the density of retinal astrocytes and vessels. In contrast to these observations, in the present study we showed that outside the macroglial retinal environment (astrocytes and Müller glial cells), *Dp71* deletion was associated with a larger angiogenic area and increased expression of VEGF in the cornea of the *Dp71*-null mice compared to the WT mice. These results may suggest that unlike in the retina, in non-physiologic circumstances, and in a tissue without vessels and astrocytes, Dp71 could act as a negative regulator of neovascularization in the cornea. This hypothesis of a role for Dp71, outside the macroglial context, was supported by the observation that in the ex vivo system of aortic rings of the *Dp71*-null mice, the angiogenic response was strongly increased, as in the cornea.

As previously mentioned, the cornea is normally devoid of blood vessels, which is important for maintaining cornea clarity. Basement membranes are cell-associated matrices that cover the basal aspect of endothelial cells. During the neoangiogenic process, the corneal ECM provides critical support to the vascular endothelium. The heterotrimeric laminins are a defining component of all basement membranes, and self-assemble into a cell-associated network. They are major structural elements of all basement membranes, but they also serve as signaling molecules through their interactions with cell surface signaling receptors, including integrins and dystroglycan [13].

We have previously reported that in the absence of Dp71, dystroglycan expression is partially inhibited in the retina,

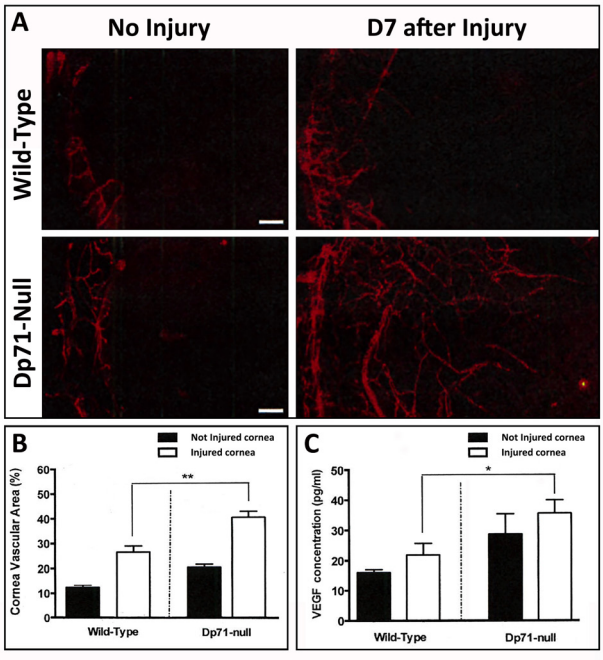

Figure 3. Corneal vascularization after or in the absence of injury. **A**: Visualization of vascular endothelial cells in flatmounted corneas using an anti-CD31 antibody conjugated with fluorescein isothiocyanate (FITC) of wild-type (WT) or *Dp71*-null mice, in the absence of injury or 7 days after injury (scale bar=200 µm). **B**: The corneal vascular area was quantified in WT or *Dp71*-null mice, in the absence of injury or 7 days after injury. **C**: The vascular endothelial growth factor (VEGF) concentration was measured with enzyme-linked immunosorbent assay (ELISA) in WT or *Dp71*-null mice, in the absence of injury or 7 days after injury.

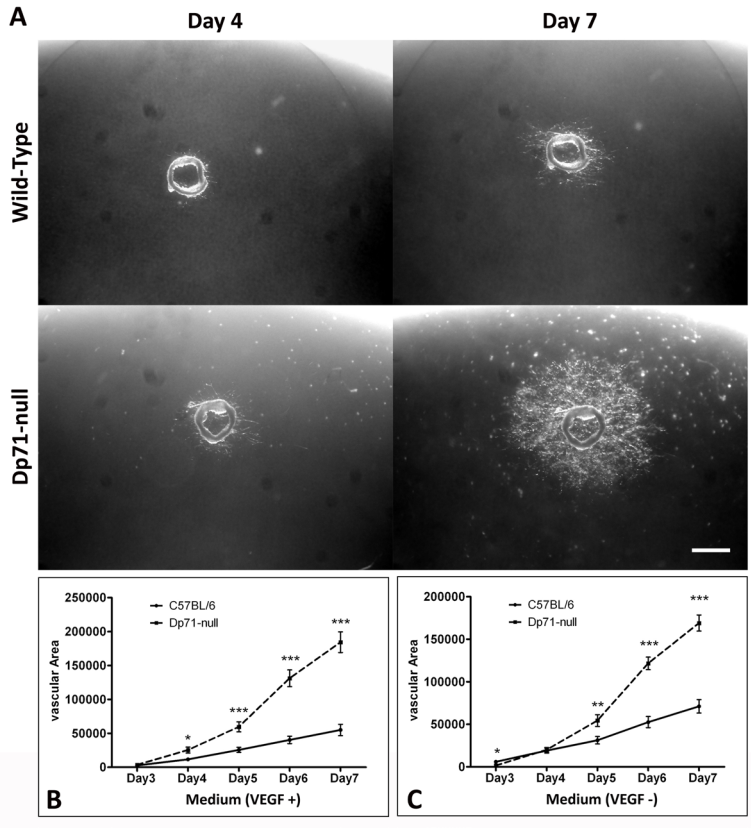

Figure 4. Role of Dp71 in angiogenesis using an aortic ring mouse model. **A**: Phase contrast photography of typical aortic rings of wild-type (WT; top) and *Dp71*-null mice (bottom) with neovessels at day 4 (left) and day 7 (right). A visible difference is already present at day 4, and will increase until day 7 (scale bar=200 µm). **B, C**: Surface covered by microvessels (in pixels) according to the time (day 3 to 7) in each group in the presence (**B**) or the absence of vascular endothelial growth factor (VEGF; **C**). Stars represent statistically significant differences (*p<0.05, **p<0.005, ***p<0.001).

laminins are impaired, and the organization of the ECM and the basement membrane is significantly altered [14,15]. Previous studies have shown that dystroglycan is detected in mouse corneal basement membranes [16], and more recently, the crucial role of laminin-8 has been reported in the increase in corneal neoangiogenesis in a *Lama4*-null mouse model [13]. Based on these observations, it could be assumed that in the cornea, the absence of *Dp71* could (i) induce the partial or total inhibition of dystroglycan expression and (ii) result in laminin disorganization. It could be proposed that the perturbation of laminins could lead to an imbalance between factors promoting vessel maturation and factors promoting endothelial cell migration and proliferation. VEGF is a key pathological feature of corneal neoangiogenesis, as suggested by the stimulatory effect of exogenous VEGF on this process, and a neutralizing effect of an anti-VEGF antibody [17]. We previously reported that the retinal expression of VEGF is upregulated in the absence of *Dp71*. The increased VEGF expression found in the injured corneas of the *Dp71*-null mice compared to the WT mice supports a stimulatory effect in the absence of Dp71 via a VEGF pathway. However, unlike what we observed in the retina where we clearly demonstrated that even when VEGF expression is increased, no increase in normal angiogenesis is observed [6], in the case of corneal injury, the increase in VEGF was associated, as expected, with an increase in neoangiogenesis. In the retina, the deletion of *Dp71* was also associated with increased retinal VEGF expression and rarefaction of retinal astrocytes, suggesting that the absence of the Dp71 protein leads to increased Müller cell–derived VEGF expression as a compensatory mechanism of the decrease in astrocytes-derived VEGF [6], and was not involved in the delay of vascular growth in the *Dp71*-null mice compared to the WT mice.

Finally, another hypothesis may be suggested: The increase of vacuoles (Figure 1) in endothelial cells, and the main localization of Dp71 in the endothelium of the cornea, could suggest an endothelium dysfunction in this model. One of the two main roles of corneal endothelial cells is a pump function, which is mediated by an active (Na^+/K+-ATPase) pump [18]. Corneal endothelial decompensation leads to overhydration of the cornea, known as corneal edema. Moreover, long-standing corneal edema also predisposes to complications, including corneal vascularization.

The mouse aortic ring model is one of the most popular models for studying angiogenesis. The signaling pathways can be assessed separately from the endothelium or the

smooth muscle. Using the X-Gal staining method, we found that Dp71 was expressed in the muscle fibers of the aortic rings. This result confirmed a previous observation that Dp71 is also expressed in human artery smooth muscle cells [19]. Although a more detailed analysis of the mechanisms regulating angiogenesis in an in vivo system (such as corneal injury) and an ex vivo system (in the aortic ring model) could show some differences, the absence of Dp71 increased angiogenesis in both models. As in the cornea model, because laminins are also expressed in the aortic rings, we could hypothesize that a similar pathway could lead to a similar phenotype. The role of VEGF should also be noted. It is known, as in the cornea model, that cultured aortic rings generate vessel sprouts without the need for exogenous growth factors, including VEGF, because their levels inside the rings are strongly increased [20]. To support this observation, we observed in the aortic model that the increase in neoangiogenesis in the WT or *Dp71*-null mice was not stimulated by the addition of exogenous VEGF (Figure 4).

Among the dystrophins produced by the *DMD* gene in the WT corneas observed with western blotting, we showed, using a pan-specific anti-dystrophin antibody, that three were expressed: Dp140, Dp116, and Dp71. We observed that the absence of *Dp71* induced an increase in Dp116 protein expression in non-injured and injured corneas (only statistically significant in the non-injured corneas), but Dp140 expression was unchanged. Dp116 is a *DMD* gene product specifically expressed in Schwan cells forming a DAP complex [21,22] similar to Dp71 in the retina. The physiologic role and the clinical phenotype of Dp116 are poorly understood, possibly because of its strong homology with other *DMD* gene products, and its expression in specific tissues [23]. Although we clearly showed that the absence of Dp71 in the cornea increased Dp116 expression, there was no functional compensation of the Dp71 phenotype observed.

In conclusion, we assessed the expression of Dp71 in mouse corneas,+ and confirmed that it was also expressed in aortic walls. We identified a new role for the dystrophin protein Dp71 in two neoangiogenesis models. Using *Dp71*-null mice, we found that Dp71 could be a negative regulator of neoangiogenesis, and that in the absence of the protein, the balance switched to enhanced angiogenesis.

APPENDIX 1.

To access the data, click or select the words "Appendix 1." Corneal surface evolution at day 3, 7 and 14 after epithelial alkaline injury in wild-type and Dp71 null mice.

APPENDIX 2.

To access the data, click or select the words "Appendix 2." Dp71 location and expression in mouse aortas. (A1) External side of a whole Dp71 null mouse aorta: positive β-Gal cells (blue) are organized perpendicularly to the vessel axis. (A2) Same aorta in cross-section: labeled cells are arranged concentrically compared to the vessel lumen. (A3) WT mouse aorta in cross-section: no cell positive for β-Gal. (B) Western-blot analysis shows Dp71 protein expression in WT aortic rings and its absence in Dp71 null aortic rings.

ACKNOWLEDGMENTS

Conflict of interest: Ramin Tadayoni is a board member of and consultant for Alcon, Switzerland; Novartis, Switzerland; Allergan, USA; Bausch and Lomb, USA; Alimera, USA; Bayer, Germany; FCI-Zeiss, France; Thrombogenics, Belgium; Roche, Switzerland; Genentech, USA; Zeiss, Germany. He received lecture fees from Alcon, USA; Bausch and Lomb, USA; Novartis, Switzerland; Allergan, USA; Bayer, Germany; Alimera, USA, Zeiss, Germany, and meeting expenses from Novartis, Switzerland; Alcon, Switzerland; Allergan, USA; Bausch and Lomb, USA; Bayer, Germany; Alimera, USA. **Audrey Giocanti-Auregan** is consultant for Allergan, USA; Bayer, Germany, and Novartis, Switzerland. She received lecture fees from Novartis, Switzerland; Allergan, USA; Bayer, Germany, and meeting expenses from Novartis, Switzerland; Alcon, Switzerland; Allergan, USA; Bayer, Germany, and Alimera, USA.

REFERENCES

1. Blake DJ, Weir A, Newey SE, Davies KE. Function and genetics of dystrophin and dystrophin-related proteins in muscle. Physiol Rev 2002; 82:291-329. [PMID: 11917091].
2. Tadayoni R, Rendon A, Soria-Jasso LE, Cisneros B. Dystrophin Dp71: the smallest but multifunctional product of the Duchenne muscular dystrophy gene. Mol Neurobiol 2012; 45:43-60. [PMID: 22105192].
3. Lumeng CN, Hauser M, Brown V, Chamberlain JS. Expression of the 71 kDa dystrophin isoform (Dp71) evaluated by gene targeting. Brain Res 1999; 830:174-8. [PMID: 10350571].
4. Claudepierre T, Dalloz C, Mornet D, Matsumura K, Sahel J, Rendon A. Characterization of the intermolecular associations of the dystrophin-associated glycoprotein complex in retinal Müller glial cells. J Cell Sci 2000; 113:3409-17. [PMID: 10984432].
5. Connors NC, Kofuji P. Dystrophin Dp71 is critical for the clustered localization of potassium channels in retinal glial cells. J Neurosci 2002; 22:4321-7. [PMID: 12040037].
6. Giocanti-Auregan A, Vacca O, Bénard R, Cao S, Siqueiros L, Montañez C, Paques M, Sahel JA, Sennlaub F, Guillonneau

X, Rendon A, Tadayoni R. Altered astrocyte morphology and vascular development in dystrophin-Dp71-null mice. Glia 2016; 64:716-29. .

7. Fort PE, Darche M, Sahel J-A, Rendon A, Tadayoni R. Lack of dystrophin protein Dp71 results in progressive cataract formation due to loss of fiber cell organization. Mol Vis 2014; 20:1480-90. [PMID: 25489223].

8. El Mathari B, Sene A, Charles-Messance H, Vacca O, Guillonneau X, Grepin C, Sennlaub F, Sahel JA, Rendon A, Tadayoni R. Dystrophin Dp71 gene deletion induces retinal vascular inflammation and capillary degeneration. Hum Mol Genet 2015; 24:3939-47. .

9. Sarig R, Mezger-Lallemand V, Gitelman I, Davis C, Fuchs O, Yaffe D, Nudel U. Targeted inactivation of Dp71, the major non-muscle product of the DMD gene: differential activity of the Dp71 promoter during development. Hum Mol Genet 1999; 8:1-10. .

10. Paranthan RR, Bargagna-Mohan P, Lau DL, Mohan R. A robust model for simultaneously inducing corneal neovascularization and retinal gliosis in the mouse eye. Mol Vis 2011; 17:1901-8. [PMID: 21850164].

11. Han Y, Shao Y, Liu T, Qu Y-L, Li W, Liu Z. Therapeutic effects of topical netrin-4 inhibits corneal neovascularization in alkali-burn rats. PLoS One 2015; 10:e0122951-[PMID: 25853509].

12. Fabbrizio E, Nudel U, Hugon G, Robert A, Pons F, Mornet D. Characterization and localization of a 77 kDa protein related to the dystrophin gene family. Biochem J 1994; 299:359-65. [PMID: 8172595].

13. Thyboll J, Kortesmaa J, Cao R, Soininen R, Wang L, Iivanainen A, Sorokin L, Risling M, Cao Y, Tryggvason K. Deletion of the laminin alpha4 chain leads to impaired microvessel maturation. Mol Cell Biol 2002; 22:1194-202. .

14. Vacca O, Darche M, Schaffer DV, Flannery JG, Sahel JA, Rendon A, Dalkara D. AAV-mediated gene delivery in Dp71-null mouse model with compromised barriers. Glia 2014; 62:468-76. .

15. Vacca O, El Mathari B, Darche M, Sahel JA, Rendon A, Dalkara D. Using Adeno-associated Virus as a Tool to Study Retinal Barriers in Disease. J Vis Exp 2015; •••:98-.

16. Ueda H, Baba T, Kashiwagi K, Iijima H, Ohno S. Dystrobrevin localization in photoreceptor axon terminals and at blood-ocular barrier sites. Invest Ophthalmol Vis Sci 2000; 41:3908-14. [PMID: 11053293].

17. Roshandel D, Eslani M, Baradaran-Rafii A, Cheung AY, Kurji K, Jabbehdari S, Maiz A, Jalali S, Djalilian AR, Holland EJ. Current and emerging therapies for corneal neovascularization. Ocul Surf 2018; 16:398-414. .

18. Feizi S. Corneal endothelial cell dysfunction: etiologies and management. Ther Adv Ophthalmol 2018; 10:2515841418815802-[PMID: 30560230].

19. Palma-Flores C, Ramírez-Sánchez I, Rosas-Vargas H, Canto P, Coral-Vázquez RM. Description of a utrophin associated protein complex in lipid raft domains of human artery smooth muscle cells. Biochim Biophys Acta 2014; 1838:1047-54. [PMID: 24060563].

20. Nicosia RF. The aortic ring model of angiogenesis: a quarter century of search and discovery. J Cell Mol Med 2009; 13:4113-36. [PMID: 19725916].

21. Yoshida M, Hama H, Ishikawa-Sakurai M, Imamura M, Mizuno Y, Araishi K, Wakabayashi-Takai E, Noguchi S, Sasaoka T, Ozawa E. Biochemical evidence for association of dystrobrevin with the sarcoglycan-sarcospan complex as a basis for understanding sarcoglycanopathy. Hum Mol Genet 2000; 9:1033-40. .

22. Hnia K, Hugon G, Masmoudi A, Mercier J, Rivier F, Mornet D. Effect of beta-dystroglycan processing on utrophin/Dp116 anchorage in normal and mdx mouse Schwann cell membrane. Neuroscience 2006; 141:607-20. [PMID: 16735092].

23. Matsuo M, Awano H, Matsumoto M, Nagai M, Kawaguchi T, Zhang Z, Nishio H. Dystrophin Dp116: A Yet to Be Investigated Product of the Duchenne Muscular Dystrophy Gene. Genes (Basel) 2017; •••:8-.

Articles are provided courtesy of Emory University and the Zhongshan Ophthalmic Center, Sun Yat-sen University, P.R. China. The print version of this article was created on 14 November 2019. This reflects all typographical corrections and errata to the article through that date. Details of any changes may be found in the online version of the article.